Variational and robust density fitting of four-center two-electron integrals in local metrics

Simen Reine,[1,a)] Erik Tellgren,[1] Andreas Krapp,[1] Thomas Kjærgaard,[1,b)] Trygve Helgaker,[1] Branislav Jansik,[2] Stinne Høst,[2] and Paweł Salek[3]
[1]*Centre of Theoretical and Computational Chemistry, Department of Chemistry, University of Oslo, P.O. Box 1033 Blindern, N-0315 Oslo, Norway*
[2]*Lundbeck Foundation Center for Theoretical Chemistry, Department of Chemistry, University of Århus, DK-8000 Århus C, Denmark*
[3]*Laboratory of Theoretical Chemistry, The Royal Institute of Technology, Teknikringen 30, Stockholm SE-10044, Sweden*

(Received 20 May 2008; accepted 18 June 2008; published online 8 September 2008)

Density fitting is an important method for speeding up quantum-chemical calculations. Linear-scaling developments in Hartree–Fock and density-functional theories have highlighted the need for linear-scaling density-fitting schemes. In this paper, we present a robust variational density-fitting scheme that allows for solving the fitting equations in local metrics instead of the traditional Coulomb metric, as required for linear scaling. Results of fitting four-center two-electron integrals in the overlap and the attenuated Gaussian damped Coulomb metric are presented, and we conclude that density fitting can be performed in local metrics at little loss of chemical accuracy. We further propose to use this theory in linear-scaling density-fitting developments. © *2008 American Institute of Physics*. [DOI: 10.1063/1.2956507]

I. INTRODUCTION

In molecular electronic-structure theory, an essential step is the evaluation of two-electron integrals over one-electron basis functions, typically taken to be linear combinations of atomic orbitals or other local or semilocal basis functions. Examples of such semilocal basis functions are Gaussian-type orbitals (GTOs) and Slater-type orbitals (STOs). The expansion coefficients are found by applying the variation principle, which ensures that all first-order variations in the energy with respect to the variations in the density are zero. Although a finite basis-set expansion may introduce quite large absolute errors, the variational property leads to high accuracy in the calculated chemical properties.

In a similar fashion, the product of two such basis functions may again be expanded in one-center auxiliary orbitals. Such density-fitting or resolution-of-the-identity (RI) approximations are introduced to speed up calculations involving four-center two-electron integrals, the traditional bottleneck of *ab initio* and density-functional calculations. In effect, the evaluation of four-center two-electron integrals is replaced by the evaluation of two- and three-center two-electron integrals and the solution of a set of linear equations. The speed-up resulting from this approach depends on the system studied and the basis set used; typically, a speed-up by a factor of 3–30 is observed.[1] The auxiliary basis sets introduced for density fitting are about three times larger than the regular basis set, while the errors introduced by the auxiliary basis are about two orders of magnitude smaller than the errors introduced by the regular basis. In this paper, we employ the auxiliary basis sets developed in Refs. 2 and 3.

The next section gives an introduction to density fitting. Next, in Sec. III, we present a robust variational scheme for approximating four-center two-electron integrals in a non-Coulomb metric, demonstrating how it can be used for the two-electron Coulomb and exchange contributions appearing in Hartree–Fock (HF) theory and Kohn–Sham (KS) density-functional theory. Implementational details are given in Sec. IV, whereas results are presented and discussed in Sec. V. Section VI contains some concluding remarks.

II. DENSITY FITTING

Density fitting was introduced independently in the Coulomb metric by Whitten[4] and in the overlap metric by Baerends *et al.*[5] In Ref. 4, Whitten established bounds on individual integrals, and later Jafri and Whitten[6] applied density fitting in self-consistent field (SCF) calculations, where individual integrals are either fitted or calculated directly depending on whether the predicted error in the fit is below a certain threshold or not. In the paper by Baerends *et al.*,[5] the electron density $\rho(\mathbf{r})$ is approximated by an expansion in atom-centered auxiliary basis functions $\xi_\alpha(\mathbf{r})$,

$$\rho(\mathbf{r}) = \sum_{ab} D_{ab}\chi_a(\mathbf{r})\chi_b(\mathbf{r}) = \sum_{ab} D_{ab}\Omega_{ab}(\mathbf{r}) \approx \tilde{\rho}(\mathbf{r}) = \sum_{\alpha}^{N_{\text{aux}}} c_\alpha \xi_\alpha(\mathbf{r}). \quad (1)$$

a)Electronic mail: simen.reine@kjemi.uio.no.
b)Permanent address: Lundbeck Foundation Center for Theoretical Chemistry, Department of Chemistry, University of Århus, DK-800 Århus C, Denmark.

Here tilde denotes a density-fitted quantity, the D_{ab} are the matrix elements of the electron density expanded in the atomic orbitals (AOs) $\chi_a(\mathbf{r})$, $\Omega_{ab}(\mathbf{r})$ is the product (overlap distribution) between $\chi_a(\mathbf{r})$ and $\chi_b(\mathbf{r})$, and c_α are the fitting coefficients. The fitted density $\tilde{\rho}(\mathbf{r})$ is used to construct an approximate Coulomb potential

$$V_C(\mathbf{r}_1) = \int \frac{\rho(\mathbf{r}_2)}{r_{12}} d\mathbf{r}_2 \approx \tilde{V}_C(\mathbf{r}_1) = \int \frac{\tilde{\rho}(\mathbf{r}_2)}{r_{12}} d\mathbf{r}_2, \tag{2}$$

which is in turn used for the construction of the Coulomb part of the Fock or KS matrix

$$\tilde{J}_{ab} = \int \Omega_{ab}(\mathbf{r}) \tilde{V}_C(\mathbf{r}) d\mathbf{r} = \int \Omega_{ab}(\mathbf{r}_1) \frac{1}{r_{12}} \tilde{\rho}(\mathbf{r}_2) d\mathbf{r}_1 d\mathbf{r}_2. \tag{3}$$

Baerends *et al.* obtained the fitting coefficients c_α by minimizing the fitting error

$$D_w = \langle \rho - \tilde{\rho} | w | \rho - \tilde{\rho} \rangle, \tag{4}$$

in the overlap metric, $w(\mathbf{r}_1, \mathbf{r}_2) = \delta(\mathbf{r}_1 - \mathbf{r}_2)$. We here use the notation

$$\langle f | w | g \rangle = \int f(\mathbf{r}_1) w(\mathbf{r}_1, \mathbf{r}_2) g(\mathbf{r}_2) d\mathbf{r}_1 d\mathbf{r}_2. \tag{5}$$

The fitted density is further constrained to conserve charge,

$$\int \rho(\mathbf{r}) d\mathbf{r} = \int \tilde{\rho}(\mathbf{r}) d\mathbf{r} = N_e, \tag{6}$$

where N_e is the number of electrons, leading to the following set of linear equations for the fitting coefficients

$$\sum_\beta \langle \alpha | w | \beta \rangle c_\beta = \sum_{cd} \langle \alpha | w | cd \rangle D_{cd} + (\alpha)\lambda, \tag{7}$$

with the Lagrange multiplier

$$\lambda = \frac{N_\mathbf{e} - \Sigma_{\alpha\beta}(\alpha)(\alpha|\beta)^{-1}(\beta|\rho)}{\Sigma_{\alpha\beta}(\alpha)(\alpha|\beta)^{-1}(\beta)}. \tag{8}$$

We use the notation $(f|g) \equiv \langle f | 1/r_{12} | g \rangle$,

$$(f|g) = \int f(\mathbf{r}_1) \frac{1}{r_{12}} g(\mathbf{r}_2) d\mathbf{r}_1 d\mathbf{r}_2 \tag{9}$$

and

$$(\alpha) = \int \xi_\alpha(\mathbf{r}) d\mathbf{r}. \tag{10}$$

The density-fitting scheme of Baerends *et al.* was further developed by Dunlap *et al.*,[7,8] who replaced the overlap operator, $\delta(\mathbf{r}_1 - \mathbf{r}_2)$, with the Coulomb operator, $1/r_{12}$. In these two papers, Dunlap *et al.* established that the Coulomb metric is superior to the overlap metric, noting that the error in the energy is about one order of magnitude smaller in the Coulomb metric than in the overlap metric.

A. Linear-scaling density fitting

Density fitting offers significant speed-ups for the calculation of four-center integrals at little loss of accuracy. Recent developments toward large systems have highlighted the need for a linear-scaling density-fitting scheme. We note that the fitting equations [Eq. (7)] in the Coulomb metric cannot be solved straightforwardly for large systems, as the computational time scales cubically with system size. In this section, we give a brief overview of different linear-scaling density-fitting schemes presented in the literature. We first discuss methods based on the spatial partitioning of electron density; next, we consider methods based on the use of a local metric.

The partitioning approach has been explored by several authors;[1,9–11] all of them effectively enforce sparsity of the solved fitting equations in different ways. In the paper by Gallant and St-Amant,[9] the density is partitioned using Yang's scheme.[12] Each of these densities is fitted separately by including fitting functions within some predefined vicinity of the density. The fitted density is further constrained to preserve charge. The resulting errors are small, but the fitted density is not variational and the procedure does not provide a continuous potential energy surface. The same is true for the method presented by Salek *et al.* in Ref. 10, although here the energy is correct to second order.

In the partitioning approach by Fonseca Guerra *et al.*,[11] the density is partitioned into diatomic densities, generated by overlaps between basis functions centered on two atoms. The diatomic densities are fitted in the overlap metric subject to charge conservation. The resulting energy is neither variational nor correct to second order. It is worth noting that STOs are used rather than GTOs and that the fitted density is used to build an approximate Coulomb potential that is included in the numerical evaluation together with the exchange-correlation contribution.

In the partitioning approach known as local atomic density fitting (LADF) or atomic resolution of the identity (ARI), Sodt *et al.*[1] partition the density into atomic regions by localizing the individual product overlaps between two basis functions to one of the two atoms that the basis functions originate from. These atomic densities are fitted individually by including fitting functions in some predefined vicinity of the atom and by introducing a bump function on the boundary to turn off smoothly which fitting functions to include. The bump function is important in order for the potential energy surface to be continuous. By including first-order Dunlap corrections,[13] the fitted energy is made variational.

Of the above partitioning schemes, the LADF scheme offers the most elegant and balanced way to obtain the fitted density, although the bump function does represent an artifact. Clearly, in all partitioning schemes, some cutoff scheme must be adopted. A criticism of these partitioning schemes is that impact of the fitting error on the calculated energies is difficult to predict.

We now turn our attention to fitting methods based on the use of a local metric.[5,14,15] In the approach of Baerends *et al.*,[5] the electron density is fitted in the overlap metric, giving errors one order of magnitude greater than in the Coulomb metric.[7] This result was confirmed by Vahtras *et al.*,[14] who compare three different ways of fitting the four-center integrals in the overlap metric to the corresponding fit in the Coulomb metric. In the paper by Jung *et al.*,[15] the expansion coefficients obtained in the Coulomb metric, the overlap

metric, and the complementary error-function attenuated metric $w(\mathbf{r}_1,\mathbf{r}_2)=\mathrm{erfc}(\omega r_{12})/r_{12}$ are compared. The attenuated metric bridges the Coulomb and the overlap metrics by varying the value of the damping parameter ω. The coefficients obtained in the overlap metric decay more or less exponentially with distance, whereas the coefficients obtained in the Coulomb metric decay more slowly at long distances. For a one-dimensional test system studied in that paper, the fitting coefficients decay as $\sim r^{-1.25}$ in the Coulomb metric, with a faster decay observed for two- and three-dimensional systems. The authors further provide statistics on atomization energies for the G2 benchmark set using RI second-order Møller–Plesset perturbation theory in the cc-pVDZ basis, reporting errors six to seven times larger in the overlap metric than in the Coulomb metric.

The scheme of Jung *et al.*[15] is neither robust nor variational. In Sec. II D, we present an extended scheme that is both robust and variational, providing an accurate and reliable linear-scaling density-fitting alternative to the LADF scheme by Sodt *et al.*[1]

B. Density-fitting exchange

Density fitting was originally introduced to approximate the full density $\rho(\mathbf{r})$ and in this way accelerate Coulomb evaluation. Similar methodology can be used in the exchange part and is also here termed density-fitting or RI approximations.

The exact-exchange matrix is given by

$$K_{ab}=\sum_{cd}(ac|bd)D_{cd}=\sum_{i}(ai|bi). \tag{11}$$

Subscript i here denotes an occupied molecular orbital (MO) $\phi_i(\mathbf{r})$, expanded in AOs with coefficients C_{ai},

$$\phi_i(\mathbf{r})=\sum_a C_{ai}\chi_a(\mathbf{r}). \tag{12}$$

The density-matrix elements D_{ab} are related to the MO coefficients according to

$$D_{ab}=\sum_i C_{ai}C_{bi}^{*}. \tag{13}$$

Density fitting of the exact exchange was introduced by Weigend.[2] In this paper, the exchange matrix of Eq. (11) was approximated as

$$\begin{aligned}\tilde{K}_{ab}&=\sum_{cd}\sum_{\alpha\beta}(ac|\alpha)(\alpha|\beta)^{-1}(\beta|bd)D_{cd}\\&=\sum_{cd}\sum_{\alpha'}(ac|\alpha')(\alpha'|bd)D_{cd},\end{aligned} \tag{14}$$

where the last step constitutes a transformation to an orthogonal auxiliary basis

$$\xi_{\alpha'}(\mathbf{r})=\sum_{\alpha}(\alpha'|\alpha)^{-1/2}\xi_\alpha(\mathbf{r}). \tag{15}$$

C. Linear-scaling density fitting of exchange

Linear-scaling aspects of density fitting in the evaluation of exchange contribution were first considered by Polly *et al.*[16] The fitted exchange matrix,

$$\tilde{K}_{ab}=\sum_i(ai|\alpha)c_\alpha^{bi}, \tag{16}$$

is computed in linear time. This is achieved using localized orbitals $\chi_a(\mathbf{r})$ and $\phi_i(\mathbf{r})$ that interact with auxiliary functions $\xi_\alpha(\mathbf{r})$ only in some local domain. Localization of the MOs is achieved through the Pipek–Mezey localization.[17] The density-fitted exchange energy,

$$\tilde{K}=\sum_{ij}\sum_{\alpha}(ij|\alpha)c_\alpha^{ij}, \tag{17}$$

is computed without use of local fitting domains. It is argued that the fitted exchange energy depends sensitively on the size of the fitting domains, whereas the optimized MO coefficients do not—reported errors are in the microhartree range. In effect the MOs are not optimized variationally, although the energy is corrected through first order. It should be noted that the final step of Eq. (17) does not scale linearly with system size, i.e., without the use of local fitting domains.

The ARI exchange method (ARI-K) of Sodt *et al.*[18] is an extension of the LADF or ARI approach of Ref. 1, applied to the exchange rather than the Coulomb contribution. In this approach, the product overlaps $\Omega_{ai}(\mathbf{r})$ are approximated by auxiliary basis functions $\xi_\alpha(\mathbf{r})$ in the local domain $[A]$ near the parent atom of AO $\chi_a(\mathbf{r})$,

$$\tilde{\Omega}_{ai}(\mathbf{r})=\sum_{\alpha\in[A]}c_\alpha^{ai}\xi_\alpha(\mathbf{r}), \tag{18}$$

with

$$c_\alpha^{ai}=\sum_{\beta\in[A]}(\alpha|\beta)_A^{-1}(\beta|ai). \tag{19}$$

As in the LADF scheme, continuity of the potential energy surface is ensured by the use of individual inverses $(\alpha|\beta)_A^{-1}$ associated with the centers A (see Ref. 18 for details). The exchange matrix of Eq. (11) is further approximated according to

$$\tilde{K}_{ab}=\frac{1}{2}\sum_i\left(\sum_{\alpha\in[A]}c_\alpha^{ai}(\alpha|bi)+\sum_{\beta\in[B]}(ai|\beta)c_\beta^{bi}\right). \tag{20}$$

We note that this approach is nonvariational, which is justified by reporting errors in energies using Eq. (20) that are typically only twice those of regular density fitting of exchange.

D. Local robust and variational fitting of four-center integrals

Let us consider the robust and variational fitting of the two-electron integrals $(ab|cd)$ in a general metric. We denote the fitted overlap distributions and their (negative) errors by

$$\widetilde{\langle ab|}=\sum_\alpha c_\alpha^{ab}\langle\alpha|,\quad \langle\Delta ab|=\langle ab|-\widetilde{\langle ab|}, \tag{21}$$

$$\widetilde{|cd\rangle} = \sum_{\beta} c_{\beta}^{cd}|\beta\rangle, \quad |\Delta cd\rangle = |cd\rangle - \widetilde{|cd\rangle}. \tag{22}$$

Following Dunlap,[13] a robust integral fitting is given by

$$\begin{aligned}(\widetilde{ab|cd}) &= (ab|\widetilde{cd}) + (\widetilde{ab}|cd) - (\widetilde{ab}|\widetilde{cd}) \\ &= (ab|cd) - (\Delta ab|\Delta cd),\end{aligned} \tag{23}$$

which is manifestly quadratic in the fitting errors. The fitting coefficients c_{α}^{ab} are obtained by minimizing the self-interaction energy of the fitting errors,

$$D_{abcd}^{w} = \langle \Delta ab|w|\Delta cd\rangle, \tag{24}$$

in a metric w, possibly different from the Coulomb metric, leading to the linear equations

$$\langle \Delta ab|w|\beta\rangle = 0, \quad \langle \alpha|w|\Delta cd\rangle = 0. \tag{25}$$

These equations are sparse when local metric and basis functions are used, allowing for an iterative solution in time proportional to system size. To make the integral [Eq. (23)] variational in the fitting coefficients, we use Lagrange's method of undetermined multipliers, treating Eq. (25) as constraints on the integral. Multiplying these constraints by $\bar{c}_{\alpha}^{ab}$ and $\bar{c}_{\beta}^{cd}$ and adding the resulting expressions to Eq. (23), we obtain

$$\begin{aligned}(\widetilde{ab|cd}) &= (ab|\widetilde{cd}) + (\widetilde{ab}|cd) - (\widetilde{ab}|\widetilde{cd}) - \langle \overline{ab}|w|\Delta cd\rangle \\ &\quad - \langle \Delta ab|w|\overline{cd}\rangle,\end{aligned} \tag{26}$$

in the notation

$$\langle \overline{ab}| = \sum_{\alpha} \bar{c}_{\alpha}^{ab}\langle \alpha|, \quad |\overline{cd}\rangle = \sum_{\beta} \bar{c}_{\beta}^{cd}|\beta\rangle. \tag{27}$$

Differentiating Eq. (26) with respect to the fitting coefficients and setting the result equal to zero, we obtain the following linear equations for the multipliers:

$$\langle \overline{ab}|w|\beta\rangle = (\Delta ab|\beta), \quad \langle \alpha|w|\overline{cd}\rangle = (\alpha|\Delta cd), \tag{28}$$

that must be solved to make the integrals variational in all parameters. Because of Eq. (25), these terms do not make a contribution to the unperturbed integrals [Eq. (26)]. However, they do become important for the calculation of molecular properties, as discussed in Sec. III, where we consider the linear-scaling evaluation of the two-electron contributions to molecular gradients.

III. LOCAL FITTING OF COULOMB AND EXACT EXCHANGE

The variational fitting of four-center integrals [Eq. (26)] can be applied to all *ab initio* methods. We here establish explicit expressions for this approach applied to the two-electron Coulomb and exact-exchange contributions in HF and KS theories. The developed theory allows for linear scaling robust variational density fitting of these two contributions in local metrics. We further show how this theory applies to molecular properties.

A. Coulomb energy and the Coulomb matrix

In the notation

$$|\rho\rangle = \sum_{ab} D_{ab}|ab\rangle, \tag{29}$$

the Coulomb repulsion energy is given by

$$J = \frac{1}{2}\sum_{abcd} D_{ab}(ab|cd)D_{cd} = \frac{1}{2}(\rho|\rho). \tag{30}$$

To obtain the corresponding expression with fitted integrals, we replace the integrals $(ab|cd)$ by $(\widetilde{ab|cd})$ of Eq. (26) and obtain

$$\tilde{J} = \frac{1}{2}\sum_{abcd} D_{ab}(\widetilde{ab|cd})D_{cd} = (\rho|\tilde{\rho}) - \frac{1}{2}(\bar{\rho}|\bar{\rho}) - \langle \bar{\rho}|w|\Delta\rho\rangle, \tag{31}$$

where $|\Delta\rho\rangle = |\rho\rangle - |\tilde{\rho}\rangle$ and

$$|\tilde{\rho}\rangle = \sum_{ab} D_{ab}\widetilde{|ab\rangle} = \sum_{\alpha} c_{\alpha}|\alpha\rangle, \quad c_{\alpha} = \sum_{ab} c_{\alpha}^{ab}D_{ab}, \tag{32}$$

$$|\bar{\rho}\rangle = \sum_{ab} D_{ab}|\overline{ab}\rangle = \sum_{\alpha} \bar{c}_{\alpha}|\alpha\rangle, \quad \bar{c}_{\alpha} = \sum_{ab} \bar{c}_{\alpha}^{ab}D_{ab}. \tag{33}$$

In Eq. (31), the last term vanishes by Eq. (25) but it is retained to obtain a variational expression for the fitted two-electron Coulomb repulsion energy, which is important for the calculation of, for example, molecular gradients.

The Fock/KS matrix is the first derivative of the HF/KS energy with respect to the density matrix elements. Therefore, the two-electron Coulomb contribution to the Fock/KS matrix, the Coulomb matrix, is given by

$$J_{ab} = \partial J/\partial D_{ab} = (ab|\rho). \tag{34}$$

We get the fitted Coulomb matrix by differentiation of the approximate Coulomb repulsion energy of Eq. (31) or simply by replacing the four-center integrals of Eq. (34) with the approximate integrals [Eq. (26)], giving

$$\tilde{J}_{ab} = \partial\tilde{J}/\partial D_{ab} = (ab|\tilde{\rho}) + (\widetilde{ab}|\rho) - (\widetilde{ab}|\tilde{\rho}), \tag{35}$$

where we have omitted the w terms, which do not contribute. The fitted Coulomb matrix can be calculated in linear time by standard direct integral evaluation routines, using Cauchy–Schwarz screening and the continuous fast multiple method (see, for example, Ref. 19 and references therein). A linear-scaling implementation also requires that the coefficients c_{β}^{ab} are determined as accurately as possible, with a resource usage proportional to system size, as can be achieved by solving Eq. (25) in a local metric.

B. Exchange energy and exchange contribution to Fock/KS matrix

We now turn our attention to exchange. The exchange energy is given as

$$K = \frac{1}{2}\sum_{abcd} D_{ab}(ac|bd)D_{cd} = \frac{1}{2}\sum_{ij}^{\text{occ}} (ij|ij), \tag{36}$$

where i and j denote the occupied MOs. Proceeding as for the Coulomb energy, we obtain

$$\tilde{K} = \frac{1}{2}\sum_{abcd} D_{ab}(\widetilde{ac|bd})D_{cd}$$
$$= \frac{1}{2}\sum_{ij}[2(ij|\widetilde{ij}) - (\widetilde{ij}|\widetilde{ij}) - 2\langle\overline{ij}|w|\Delta ij\rangle], \quad (37)$$

where we have introduced $|\Delta ij\rangle = |ij\rangle - |\widetilde{ij}\rangle$ and

$$|\widetilde{ij}\rangle = \sum_{\alpha} c_{\alpha}^{ij}|\alpha\rangle, \quad c_{\alpha}^{ij} = \sum_{ab} c_{\alpha}^{ab}C_{ai}C_{bj}, \quad (38)$$

$$|\overline{ij}\rangle = \sum_{\alpha} \bar{c}_{\alpha}^{ij}|\alpha\rangle, \quad \bar{c}_{\alpha}^{ij} = \sum_{ab} \bar{c}_{\alpha}^{ab}C_{ai}C_{bj}. \quad (39)$$

As for the Coulomb energy [Eq. (31)], the last term in Eq. (37) is zero but is retained since it contributes to gradients. The exchange matrix is the derivative of the exchange energy [Eq. (36)] with respect to the density-matrix elements D_{ab},

$$K_{ab} = \partial K/\partial D_{ab} = \sum_{cd}(ac|bd)D_{cd} = \sum_{i}^{\text{occ}}(ai|bi). \quad (40)$$

In the same manner as for the Coulomb energy, we obtain the density-fitted expressions for the exchange energy and matrix,

$$\tilde{K}_{ab} = \partial\tilde{K}/\partial D_{ab}$$
$$= \sum_{cd}(\widetilde{ac|bd})D_{cd}$$
$$= \sum_{i}[(ai|\widetilde{bi}) + (\widetilde{ai}|bi) - (\widetilde{ai}|\widetilde{bi})], \quad (41)$$

where the notation for $|\widetilde{ai}\rangle$ and $|\overline{ai}\rangle$ is analogous to that of Eqs. (38) and (39). When the fitting coefficients c_{α}^{ai} are obtained in the Coulomb metric, the last two terms vanish to give the expression of the fitted exchange matrix of Polly *et al.*[16] given by Eq. (16).

The density-matrix elements couple basis functions on the two electrons. This coupling, together with screening, is exploited for insulators in the order-N exchange[20] and in the linear-scaling exchange[21] (LinK) algorithms to achieve linear scaling with system size in Eq. (40). An alternative approach is to use localized molecular orbitals (LMOs) (see Ref. 22 and references therein). Linear scaling then follows by using these LMOs and Cauchy–Schwarz screening since, provided that the AOs χ_a and χ_b are sufficiently far away from each other, a given LMO will not overlap with both AOs. To see this, we apply the Cauchy–Schwarz inequality twice,

$$|(ai|bi)| \leqslant \sqrt{(ai|ai)}\sqrt{(bi|bi)}$$
$$\leqslant \left[\sum_{c}|C_{ci}|\sqrt{(ac|ac)}\right]\left[\sum_{c}|C_{ci}|\sqrt{(bc|bc)}\right], \quad (42)$$

where we have used

$$(ai|ai) = \sum_{cd} C_{ci}C_{di}(ac|ad)$$
$$\leqslant \sum_{cd}|C_{ci}||C_{di}|\sqrt{(ac|ac)}\sqrt{(ad|ad)}$$
$$= \left[\sum_{c}|C_{ci}|\sqrt{(ac|ac)}\right]^2, \quad (43)$$

and so on.

For insulators, linear-scaling density-fitted exchange-matrix construction can be achieved in a local metric by following the same arguments as for the regular exchange matrix and by pretabulating which three-center Coulomb repulsion integrals $(ab|\alpha)$ [or $(ai|\alpha)$] to calculate. First, we note that, in a local metric, the number of fitting coefficients c_{α}^{ab} scales linearly with system size, as auxiliary basis functions $\xi_{\alpha}(\mathbf{r})$ sufficiently far away from the product overlaps $\Omega_{ab}(\mathbf{r})$ do not contribute to the fitted product overlap $\tilde{\Omega}_{ab}(\mathbf{r})$.[15] Second, since D_{cd} couple basis functions on two different electrons, $\chi_c(\mathbf{r}_1)$ and $\chi_d(\mathbf{r}_2)$, we can neglect all integrals $(ac|bd)$ where the density-matrix elements become sufficiently small for example, using Cauchy–Schwarz screening

$$|(ac|bd)D_{cd}| \leqslant \sqrt{(ac|ac)}\sqrt{(bd|bd)}|D_{cd}|. \quad (44)$$

Therefore, the fitted integrals $(\widetilde{ac|bd})$ of $(ac|bd)$ need only be calculated whenever

$$\sqrt{(ac|ac)}\sqrt{(bd|bd)}|D_{cd}| \geqslant \epsilon, \quad (45)$$

for a given threshold ϵ. For insulators, the density-matrix elements decrease in magnitude with increasing distance, which means, for instance, that $\Omega_{ac}(\mathbf{r}_1)$ only interact with $\tilde{\Omega}_{bd}(\mathbf{r}_2)$ provided that $\chi_c(\mathbf{r}_1)$ and $\chi_d(\mathbf{r}_2)$ are within some finite distance of each other. As a result, $\chi_a(\mathbf{r}_1)$ and $\chi_b(\mathbf{r}_2)$ must also be close to each other. The same argument applies to the fitting functions since $\xi_{\alpha}(\mathbf{r}_2)$, included in $\tilde{\Omega}_{bd}(\mathbf{r}_2)$, have a limited extent from the center of $\Omega_{bd}(\mathbf{r}_2)$, from which $\tilde{\Omega}_{bd}(\mathbf{r}_2)$ originates. The combined effects of locality in the density matrix and locality in the fit imply that the number of contributing three-center integrals $(ac|\alpha)$ scales linearly with system size. The same argument holds for the two-center integrals appearing in the last term of Eq. (41).

C. Contributions to gradient

To conclude this section, we make a note on how to achieve linear scaling for the exchange contribution when calculating properties (such as the molecular gradient) that involve explicit differentiation of the four-center integrals $(ac|bd)$. Let η denote some variable, for example, a nuclear coordinate. Differentiation of the fitted exchange energy of Eq. (37) with respect to η gives

$$\frac{d\tilde{K}}{d\eta} = \sum_{ab} D_{ab}^{\eta}\tilde{K}_{ab} + \sum_{ab} D_{ab}\tilde{K}_{ab}^{\eta} + \sum_{ab} D_{ab}\bar{K}_{ab}^{\eta}, \quad (46)$$

with

Initialization

Non-Coulombic metric w

Construct $G^w_{ab} = \sqrt{\langle ab|w|ab\rangle}$ and $G^w_\alpha = \sqrt{\langle \alpha|w|\alpha\rangle}$

Normalize $\{\xi_\alpha\}$ in metric w (i.e. division with G^w_α)

Construct $\langle \alpha|w|\beta\rangle$ and decompose to $\langle \alpha|w|\beta\rangle^{\pm\frac{1}{2}}$

Construct $\langle ab|w|\alpha\rangle \geq G^w_{ab}G^w_\alpha = G^w_{ab}$

Orthogonalize the auxiliary basis according to $c^{ab}_{\alpha'} = \langle ab|w|\alpha'\rangle = \sum_\alpha \langle ab|w|\alpha\rangle \langle \alpha|w|\alpha'\rangle^{-\frac{1}{2}}$

Coulombic metric

Construct $G_{ab} = \sqrt{(ab|ab)}$ and $G_\alpha = \sqrt{(\alpha|\alpha)}$

Construct $(\alpha|\beta)$ and orthogonalize in metric w, $(\alpha'|\beta') = \langle \alpha'|w|\alpha\rangle^{-\frac{1}{2}}(\alpha|\beta)\langle \beta|w|\beta'\rangle^{-\frac{1}{2}}$

Construct $(ab|\alpha) \geq G_{ab}G_\alpha$

Orthogonalize according to $(ab|\alpha') = (ab|\alpha)\langle \alpha|w|\alpha'\rangle^{-\frac{1}{2}}$

Each iteration

Fitted Coulomb matrix $\tilde{J}_{ab}$

Construct $c_{\alpha'} = \sum_{cd} D_{cd}\langle cd|w|\alpha'\rangle = \sum_{cd} D_{cd}c^{cd}_{\alpha'}$

Compute intermediate $\tilde{J}^I_{ab} = \sum_{\alpha'}(ab|\alpha')c_{\alpha'}$

Construct $\gamma_{\alpha'} = \sum_{cd}(\alpha'|cd)D_{cd} - \sum_{\beta'}(\alpha'|\beta')c_{\beta'}$

Construct $\tilde{J}_{ab} = \tilde{J}^I_{ab} + \sum_{\alpha'} c^{ab}_{\alpha'}\gamma_{\alpha'}$

Fitted exchange matrix $\tilde{K}_{ab}$

Construct Cholesky MO's by Cholesky decomposition of density matrix, $D_{ab} = \sum_i^{occ} L_{ai}L_{bi}$

MO half-transform according to $c^{ai}_{\alpha'} = \sum_b c^{ab}_{\alpha'}L_{bi}$, and $(ai|\alpha') = \sum_b L_{bi}(ab|\alpha')$

Build intermediate $\tilde{K}^I_{ab} = \sum_{i\alpha'}(ai|\alpha')c^{bi}_{\alpha'}$

Build intermediate $\tilde{K}^{II}_{ab} = \tilde{K}^I_{ab} + \sum_{i\alpha'} c^{ai}_{\alpha'}(bi|\alpha')$

Finalize fitted exchange matrix $\tilde{K}_{ab} = \tilde{K}^{II}_{ab} - \sum_{i\alpha'\beta} c^{ai}_{\alpha'}(\alpha'|\beta')c^{bi}_{\beta'}$

FIG. 1. Outline of the algorithm employed for fitting the Coulomb and exchange matrices in local metrics.

$$D^\eta_{ab} = \frac{dD_{ab}}{d\eta} \tag{47}$$

and

$$\tilde{K}^\eta_{ab} = \sum_{cd}\left(\sum_\beta (\{ac\}^\eta|\beta)c^{bd}_\beta + \sum_\alpha c^{ac}_\alpha(\alpha^\eta|\Delta bd)\right)D_{cd}, \tag{48}$$

and the term including the Lagrangian multipliers

$$\bar{K}^\eta_{ab} = \sum_{cd}\left(\sum_\alpha \lambda^{ac}_\alpha[\langle \alpha^\eta|w|\Delta bd\rangle + \langle \alpha|w|\{\Delta bd\}^\eta\rangle]\right)D_{cd}. \tag{49}$$

In the last two equations the superscript η denotes differentiation with respect to η, so that, for example,

$$\langle \alpha^\eta|w|\Delta bd\rangle = \int \frac{d\xi_\alpha(\mathbf{r}_1)}{d\eta} w(\mathbf{r}_1,\mathbf{r}_2)(\Omega_{bd}(\mathbf{r}_2) - \tilde{\Omega}_{bd}(\mathbf{r}_2))d\mathbf{r}_1 d\mathbf{r}_2. \tag{50}$$

Linear scaling of the two first terms of Eq. (46) follows the same arguments as for the undifferentiated case, whereas linear scaling of the third term requires insertion of the expression for the Lagrangian multipliers of Eq. (28),

$$\bar{K}^\eta_{ab} = \sum_{cd}\left(\sum_{\alpha\beta}(\Delta ac|\alpha)\langle \alpha|w|\beta\rangle^{-1}[\langle \beta^\eta|w|\Delta bd\rangle + \langle \beta|w|\{\Delta bd\}^\eta\rangle]\right)D_{cd}. \tag{51}$$

Linear scaling can be achieved by letting the inverse $\langle \alpha|w|\beta\rangle^{-1}$ matrix work to the right rather than the left—thereby bypassing explicitly solving for the Lagrangian multipliers.

IV. IMPLEMENTATION DETAILS

Figure 1 outlines the algorithm employed in this paper for the construction of the fitted Coulomb and exchange matrices following Eqs. (35) and (41), respectively. To condition the linear set of equations optimally, we orthonormalize the auxiliary basis functions—that is, we normalize in metric w using $g^w_\alpha = \sqrt{\langle \alpha|w|\alpha\rangle}$ and orthogonalize by multiplication of the inverse square root of the auxiliary two-center integrals $\mathbf{V}^w$,

$$V^w_{\alpha,\beta} = \langle \alpha|w|\beta\rangle. \tag{52}$$

The inverse square root $(\mathbf{V}^w)^{-1/2}$ is obtained with the scheme presented in Ref. 23. In the orthogonal basis $\xi_{\alpha'} = \Sigma_\alpha \xi_\alpha \langle \alpha|w|\alpha'\rangle^{-1/2}$, we thus have

$$V^{w}_{\alpha',\beta'} = \langle \alpha' | w | \beta' \rangle = \sum_{\alpha\beta} \langle \alpha' | w | \alpha \rangle^{-1/2} \langle \alpha | w | \beta \rangle \langle \beta | w | \beta' \rangle^{-1/2} = \delta_{\alpha',\beta'}. \quad (53)$$

The three center integrals are calculated using Cauchy–Schwarz screening,

$$|\langle \alpha | w | ab \rangle| \leq g^{w}_{ab} g^{w}_{\alpha}, \quad (54)$$

with

$$g^{w}_{f} = \sqrt{\langle f | w | f \rangle}. \quad (55)$$

More specifically, we only calculate the three-center integrals $\langle \alpha | w | ab \rangle$ if $g_{ab} \geqslant \tau / g^{w}_{\alpha}$ for a given threshold τ. Furthermore, the three-center integrals are packed in triangular form to exploit the symmetry of the integrals $\langle a | w | ab \rangle = \langle \alpha | w | ba \rangle$. We do not, in the current implementation, exploit the sparsity obtained in a local metric, although, in Sec. V, we report this sparsity for a selected system.

In the orthogonal basis, the fitting coefficients of Eq. (25) reduce to the three-center integrals,

$$c^{ab}_{\alpha'} = \langle \alpha' | w | ab \rangle. \quad (56)$$

The construction of the fitted Coulomb and exchange matrices, given by Eqs. (35) and (41), respectively, follows straightforwardly by contracting the fitting coefficients with the three-center integrals $(\alpha' | ab)$ and $(\alpha' | \beta')$. However, to speed up the construction of the fitted exchange matrix, we first MO half-transform both the fitting coefficients,

$$c^{ai}_{\alpha'} = \sum_{b} c^{ab}_{\alpha'} L_{bi}, \quad (57)$$

and the three-center Coulomb repulsion integrals,

$$(ai | \alpha') = \sum_{b} (ab | \alpha') L_{bi}, \quad (58)$$

using the localized Cholesky MO coefficients L_{ai} obtained by the incomplete Cholesky decomposition of the density matrix,[22]

$$D_{ab} = \sum_{i} L_{ai} L_{bi}. \quad (59)$$

A. Integral evaluation

In this subsection, we provide a brief overview on how we evaluate the molecular integrals in the different metrics $w(\mathbf{r}_1, \mathbf{r}_2)$ used to determine the fitting coefficients of Eq. (25). Several general integration schemes are available in literature (see, for instance, Ref. 24). The current implementation is part of a development version of DALTON, in which the McMurchie–Davidson scheme forms the basis for integral evaluation.[25] In the McMurchie–Davidson scheme, the product overlap distribution between two (spherical-harmonic) basis functions is expanded in Hermite Gaussian primitives $\Lambda^{\mathbf{P}}_{tuv}(\mathbf{r})$, according to

$$\Omega_{ab}(\mathbf{r}) = \sum_{tuv} E^{ab}_{tuv} \Lambda^{\mathbf{P}}_{tuv}(\mathbf{r}), \quad \Lambda^{\mathbf{P}}_{tuv}(\mathbf{r}) = \frac{\partial^{t+u+v} e^{-p r^2_{\mathbf{P}}}}{\partial P^{t}_{x} \partial P^{u}_{y} \partial P^{v}_{z}}, \quad (60)$$

with $p = a + b$, and $\mathbf{P} = (a\mathbf{A} + b\mathbf{B})/p$ (see Ref. 24 for details).

The two electron integral between two such overlap distributions is, in metric $w(\mathbf{r}_1, \mathbf{r}_2)$, given by

$$\langle ab | w | cd \rangle = \frac{2\pi^{5/2}}{pq\sqrt{p+q}} \sum_{tuv} E^{ab}_{tuv} \times \sum_{\tau\nu\phi} (-1)^{\tau+\nu+\phi} E^{cd}_{\tau\nu\phi} W_{t+\tau,u+\nu,v+\phi}(\gamma, \mathbf{R}_{PQ}), \quad (61)$$

with $\gamma = pq/(p+q)$ and where $\mathbf{R}_{PQ}$ refers to the distance between the two overlap distributions. In this expression, only the Hermite two-electron integral,

$$W_{t,u,v}(\gamma, \mathbf{R}_{PQ}) = \frac{\partial^{t+u+v} W(\gamma, \mathbf{R}_{PQ})}{\partial P^{t}_{x} \partial P^{u}_{y} \partial P^{v}_{z}}, \quad (62)$$

depends on the metric $w(\mathbf{r}_1, \mathbf{r}_2)$ with, for example,

$$W(\gamma, \mathbf{R}_{PQ}) = \begin{cases} F_0(\gamma R^2_{PQ}) & \text{for } w(\mathbf{r}_1, \mathbf{r}_2) = 1/r_{12} \\ \gamma/(2\pi)\exp(-\gamma R^2_{PQ}) & \text{for } w(\mathbf{r}_1, \mathbf{r}_2) = \delta(\mathbf{r}_1 - \mathbf{r}_2) \\ F_0(\gamma R^2_{PQ}) - \sqrt{\delta} F_0(\gamma \delta R^2_{PQ}) & \text{for } w(\mathbf{r}_1, \mathbf{r}_2) = \mathrm{erfc}(\omega r_{12})/r_{12} \\ \kappa F_0(\kappa \gamma R^2_{PQ}) \exp(-\kappa \omega R^2_{PQ}) & \text{for } w(\mathbf{r}_1, \mathbf{r}_2) = \exp(-\omega r^2_{12})/r_{12}. \end{cases} \quad (63)$$

Here $\delta = \omega^2/(\gamma+\omega)$, $\kappa = \gamma/(\gamma+\omega)$, $F_0(x)$ is the zeroth order Boys function, and ω is the attenuation parameter. The Hermite two-electron integral $W_{t,u,v}(\gamma, \mathbf{R}_{PQ})$ can be found by reccurence.[24,26] Note that for both the attenuated Coulomb metrics of Eq. (63), the complementary error-function Coulomb metric $\mathrm{erfc}(\omega r_{12})/r_{12}$, and the Gaussian damped Coulomb metric $\exp(-\omega r^2_{12})/r_{12}$, we retain the Coulomb integrals in the limit $\omega \to 0$, whereas in the limit $\omega \to \infty$, we get scaled overlap integrals (with prefactors π/ω^2 and $2\pi/\omega$, respectively). Also note that the auxiliary basis functions used for density fitting may, similarly to the expansion of the overlap distributions Eq. (60), be expanded in Hermite

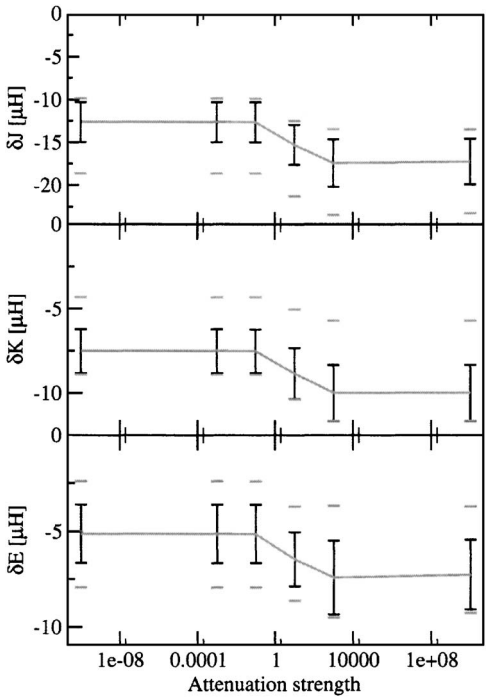

FIG. 2. Average value and standard deviations for the fitting errors in Coulomb δJ, exchange δK, and total energy δE as computed for the benchmark molecule set as a function of varying attenuation strength ω. The basis-set combination cc-pVTZ(df-pVTZ) was used. Errors are computed per nonhydrogen atom, and results were obtained using the Gaussian damped Coulomb metric $\exp(-\omega r_{12}^2)/r_{12}$. Maximal and minimal deviations are marked with bars.

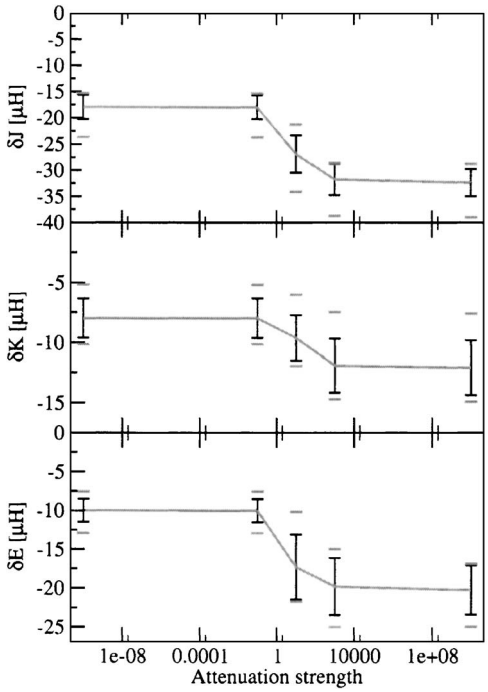

FIG. 3. Average value and standard deviations for the fitting errors in Coulomb δJ, exchange δK, and total energy δE as computed for the benchmark molecule set as a function of varying attenuation strength ω. The basis-set combination 6-31G(df-def2) was used. Errors are computed per nonhydrogen atom, and results were obtained using the Gaussian damped Coulomb metric $\exp(-\omega r_{12}^2)/r_{12}$. Maximal and minimal deviations are marked with bars.

Gaussians. Therefore, the arguments given in this subsection also apply to two-electron integrals involving auxiliary basis functions. Finally note that to speed up the integral evaluation, we use Hermite instead of Cartesian primitive functions for the auxiliary basis functions according to Ref. 27.

V. RESULTS AND DISCUSSION

To assess the presented method with respect to accuracy, we shall now examine the errors introduced in the calculated energies, atomization energies, and reaction enthalpies for a set of test systems. We demonstrate that local density fitting can be applied to molecular energies, at little cost of accuracy. We also take a look at energy differences, presenting results for both atomization energies and reaction enthalpies. The errors in energy differences are more sensitive than the errors in molecular energies when making the transition from Coulomb to overlap density fitting. Although the density-fitting errors are still small, compared to, for example, orbital basis-set errors, the somewhat larger errors for energy differences may constitute a criticism of the presented method. We therefore discuss these issues in greater detail. We finally make a note on computation performance as well as on the sparsity for different screening thresholds.

A. Molecular errors

Figures 2 and 3 display the effect of attenuation on Coulomb, exchange, and total energies at different levels of attenuation ω. Results are for the benchmark set of Ref. 28 at the B3LYP/cc-pVTZ(df-pVTZ) and B3LYP/6-31G(df-def2) levels of theory. The auxiliary basis sets used for density fitting are given in parentheses; df-pVTZ is the triple-zeta valence plus polarization basis set of Ref. 2 and df-def2 is the standard "RI-JK auxiliary basis set" of Ref. 3. Mean errors in the Coulomb δJ, exchange δK, and total energies δE for the full benchmark set are plotted together with the corresponding standard deviations, maximum errors, and minimum errors. The plots were obtained using the Gaussian damped Coulomb metric $\exp(-\omega r_{12}^2)/r_{12}$. The limit of a small ω corresponds to Coulomb fitting, while a large attenuation factor ω approaches overlap fitting. Concerning the choice of a local metric, we note that the performance of the Gaussian and error-function damping is similar with respect to size of the errors. Since Gaussian damping gives rise to more sparsity, it is recommended over error-function damping for large systems.

Inserting Eq. (23) into Eqs. (31) and (37), we obtain

$$\tilde{J} = J + \delta J = J - \tfrac{1}{2}(\Delta\rho|\Delta\rho), \tag{64}$$

$$\tilde{K} = K + \delta K = K - \frac{1}{2}\sum_{ij}(\Delta ij|\Delta ij), \tag{65}$$

and conclude that the density-fitting errors in the Coulomb and exchange energies are both negative. The sign of the total fitting error $\delta E = \delta J - \delta K$ therefore depends on the relation between the Coulomb δJ and the exchange δK errors.

In the B3LYP calculations examined here, the density-fitting error in the Coulomb contribution is larger than the error in the exchange contribution. In Hartree–Fock calcula-

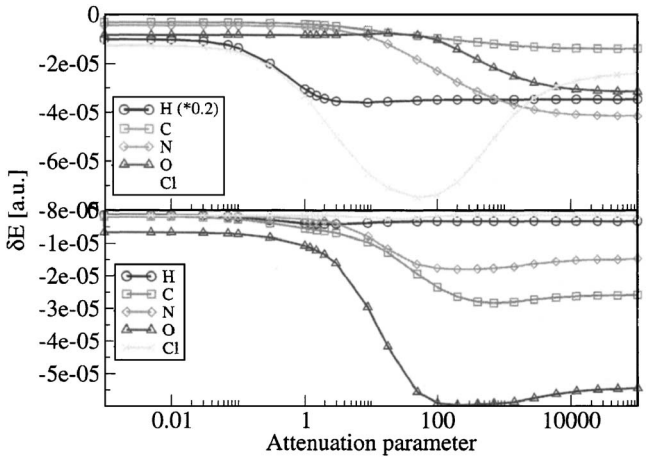

FIG. 4. Total density-fitting error δE obtained for hydrogen, carbon, nitrogen, oxygen, and chlorine atoms at B3LYP density-functional level as a function of Gaussian attenuation strength ω. Top panel displays the fitting error obtained for 6-31G(df-def2) basis-set combination—bottom panel for cc-pVTZ(df-pVTZ) combination. Error for hydrogen and 6-31G(df-def2) combination was scaled down five times.

tions, where the contribution from exact exchange is five times larger than in the B3LYP calculations, the exchange error is two to three times larger than the Coulomb error. Since the Coulomb and exchange errors are both negative, the total error is never larger than the error in one of the contributions. As seen from Figs. 2 and 3, attenuation increases the molecular fitting errors but never by more than 50%. Since the fitting errors are much smaller than the basis-set error, we conclude that attenuated local fitting can be used instead of Coulomb fitting, in molecular calculations, without adversely affecting the resulting total energies.

B. Atomic errors

In this section we address both atomic and atomization density-fitting energies. These two quantities are more sensitive than molecular energies to the transition from Coulomb to overlap density fitting. We attribute this to an auxiliary basis-set superposition error.

In Fig. 4, we have plotted the density-fitting error as a function of attenuation parameter ω for the atoms in the benchmark set.[28] Clearly, the atomic calculations behave differently from the molecular ones. In the atomic calculations, the transition from the Coulomb to the overlap metric increases the fitting error by up to a factor of 8. Moreover, the atomic errors do not increase monotonically as we approach the overlap metric. Instead, the largest fitting error occurs for some intermediate value of ω. Clearly, the attenuation error depends strongly on the auxiliary basis set.

TABLE I. Errors in atomization energies (μhartree) arising from Coulomb and overlap density fitting for N_2 and CO at the B3LYP/cc-pVTZ(df-pVTZ) level of theory, with and without use of the CP correction. The calculations have been carried out at the experimental bond distances of 109.768 pm for N_2 and 112.8323 pm for CO.

	Coulomb		Overlap	
Molecule	No CP	CP	No CP	CP
N_2	21	20	46	26
CO	22	20	52	1

In molecules, auxiliary basis functions on neighboring atoms help to lower the fitting error. These additional functions are unavailable in atomic calculations, giving an unbalanced description of atomic and molecular systems and an associated basis-set superposition error (BSSE) in the energies. The BSSE can, at least to some extent, be corrected for by application of the counterpoise (CP) correction of Ref. 29.

In the case of density fitting such a BSSE effect would be prominent due to limited flexibility of the auxiliary basis set. To examine the BSSE associated with the auxiliary basis set, we have applied the CP correction to atomization-energy calculations on N_2 and CO. The results in Table I show that auxiliary BSSE is more prominent in the overlap metric than in the Coulomb metric. In the Coulomb metric, the CP correction has little effect on the atomization energies, whereas overlap density-fitting errors are reduced from 46 to 26 μhartrees for N_2 and from 52 to 1 μhartree for CO. Clearly, the latter value is an example of a fortuitous cancellation of errors.

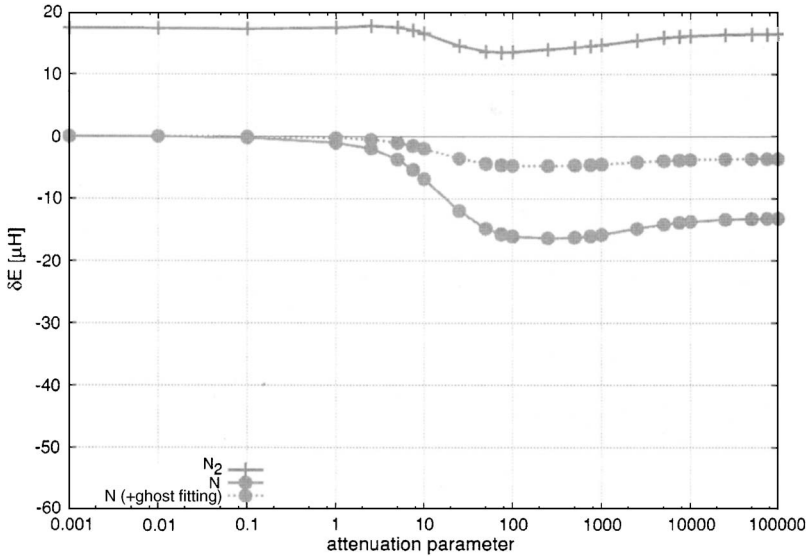

FIG. 5. Variation of the total density-fitting error δE with the attenuation parameter ω for the N_2 molecule and the N atom at B3LYP/cc-pVTZ(df-pVTZ) level of theory. The experimental bond length of 109.768 pm was used for N_2. Results were obtained using the Gaussian damped metric $\exp(-\omega r_{12}^2)/r_{12}$. The atomic calculations labeled "ghost fitting" involve regular (orbital) basis functions for one of the atoms and auxiliary basis functions at the positions of both atoms.

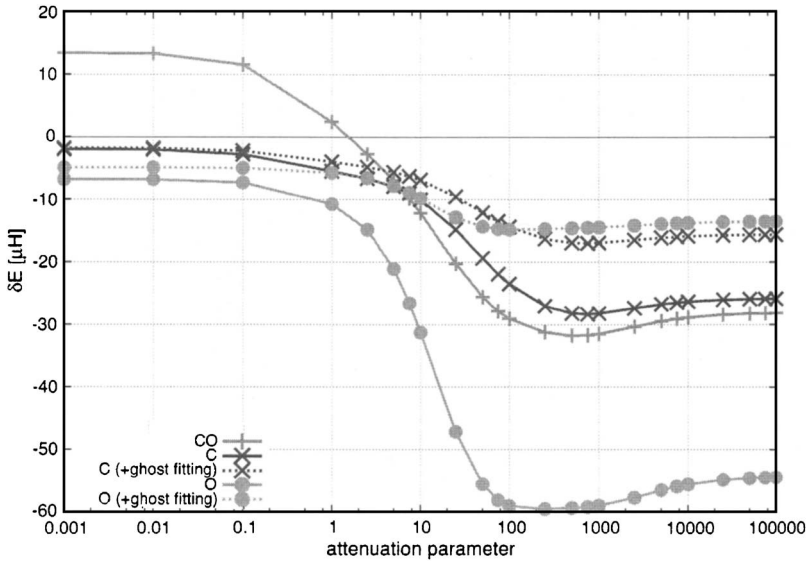

FIG. 6. Variation of the total density-fitting error δE with the attenuation parameter ω for the CO molecule and the C and O atoms at B3LYP/cc-pVTZ(df-pVTZ) level of theory. The experimental bond length of 112.8323 pm was used for CO. Results were obtained using the Gaussian damped metric $\exp(-\omega r_{12}^2)/r_{12}$. The atomic calculations labeled "ghost fitting" involve regular (orbital) basis functions for the atom in question and auxiliary basis functions at the positions of both atoms.

Figures 5 and 6 show the B3LYP/cc-pVTZ(df-pVTZ) density-fitting errors at different levels of attenuation for the two molecules, as well as atomic energies calculated with and without ghost fitting functions at the positions of the bonding partners. The atomic fitting errors are reduced substantially once the flexibility of the auxiliary basis set is enhanced. In particular, for the oxygen atom, the ratio between the overlap and Coulomb density-fitting errors is reduced from 7.7 to 2.7 when the ghost fitting functions are included. Moreover, with ghost functions in the atomic calculations, the dependency of the fitting errors of the attenuation parameter is less pronounced, as seen from the reduced slope of the corresponding curves in Figs. 5 and 6.

In summary, the BSSE is more pronounced in the attenuated and overlap metrics than in the Coulomb metric. However, we note that the auxiliary basis set used in this investigation were optimized with respect to density fitting in the Coulomb metric. The use of auxiliary basis sets optimized in the overlap metric may reduce the BSSE. However, even with the standard auxiliary basis sets used here, the density-fitting error is small compared with the orbital basis-set error.

C. Reaction energies

From a chemical point of view, relative energies are more important than total energies. To obtain reliable reaction energies for a given method, the errors of products and reactants must be balanced. We tested our approach on 11 reaction energies (A–K) at the B3LYP/6-31G(df-def2) level of theory (see Table II). The test set includes isomerization reactions (A–C), bond-breaking reactions leading to closed-shell species (D–G), and bond-breaking reactions leading to open-shell species (H–K). The geometries for all species

TABLE II. Densit-fitting errors δE (μhartree) of reaction energies for reactions A–K in the overlap and Coulomb metris. Also listed are the sum of the density-fitting error of the reactants δE_{reac} and of the products δE_{prod}. Calculations were carried out at the B3LYP/6-31G(df-def2) level of theory.

		δE		δE_{reac}		δE_{prod}	
		Over.	Coul.	Over.	Coul.	Over.	Coul.
A: $C_{12}H_{12}$ (1)	$\rightarrow C_{12}H_{12}$ (2)	66	17	−268	−144	−202	−127
B: $C_{12}H_{12}$ (1)	$\rightarrow C_{12}H_{12}$ (3)	13	25	−268	−144	−254	−119
C: $(CH_3)_3CC(CH_3)_3$	$\rightarrow n-C_8H_{18}$	−33	−21	−113	−103	−146	−124
D: $n-C_6H_{14}+4\ CH_4$	$\rightarrow 5\ C_2H_6$	37	3	−287	−199	−250	−195
E: $n-C_8H_{18}+6\ CH_4$	$\rightarrow 7\ C_2H_6$	59	5	−410	−280	−350	−273
F: adamantane	$\rightarrow 3\ C_2H_4+2\ C_2H_2$	−90	−8	−132	−117	−222	−125
G: bicyclo[2.2.2]octane	$\rightarrow 3\ C_2H_4+C_2H_2$	−63	−8	−133	−101	−195	−109
H: CH_3OCH_3	$\rightarrow CH_3O+CH_3$	29[a]	4[b]	−101[c]	−59[d]	−72[e]	−55[f]
I: $CH_3OCH_2CH_3$	$\rightarrow CH_3O+CH_2CH_3$	18[a]	4[b]	−104[c]	−70[d]	−87[e]	−66[f]
J: $CH_3OCH(CH_3)_2$	$\rightarrow CH_3O+CH(CH_3)_2$	22[a]	4[b]	−121[c]	−83[d]	−99[e]	−78[f]
K: $CH_3OC(CH_3)_3$	$\rightarrow CH_3O+C(CH_3)_3$	34[a]	10[b]	−135[c]	−95[d]	−100[e]	−85[f]

[a] δE using cc-pVTZ(df-pVTZ) for H, I, J, K: 18, 17, −0.4, and −6, respectively.
[b] δE using cc-pVTZ(df-pVTZ) for H, I, J, K: −3, −0.4, 3, and 4, respectively.
[c] δE_{reac} using cc-pVTZ(df-pVTZ) for H, I, J, K: −61, −72, −71, and −71, respectively.
[d] δE_{reac} using cc-pVTZ(df-pVTZ) for H, I, J, K: −31, −39, −47, and −53, respectively.
[e] δE_{prod} using cc-pVTZ(df-pVTZ) for H, I, J, K: −43, −54, −71, and −77, respectively.
[f] δE_{prod} using cc-pVTZ(df-pVTZ) for H, I, J, K: −34, −39, −44, and −49, respectively.

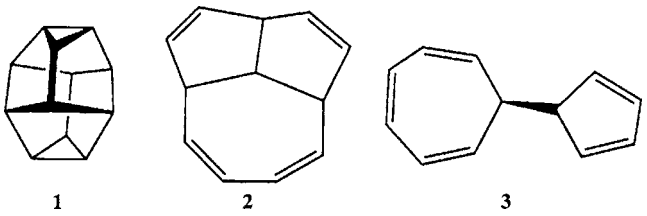

FIG. 7. Structures of three different isomers of $C_{12}H_{12}$: 1, 2, and 3.

were taken from Ref. 30. Figure 7 shows the three isomers 1–3 of $C_{12}H_{12}$ considered in reactions A and B.

The absolute values of the overlap density-fitting errors of the reaction energies are between 13 and 90 μhartrees, to be compared with the Coulomb density-fitting errors between 3 and 25 μhartrees. Moreover, the fitting errors in reaction energies are typically one order of magnitude smaller than the total fitting errors of the products and reactants. A comparison of the fitting errors in the overlap and Coulomb metric reveals that both approaches differ less for isomerization reactions than for bond-breaking reactions, as expected from the interpretation that the fitting error in the overlap metric suffers from BSSE. A reduction in the absolute value of the fitting error is observed when switching from the small 6-31G(df-def2) to the large cc-pVTZ(df-pVTZ) basis set. The very small overlap fitting errors for reaction I (0.4 μhartree) and the Coulomb fitting error for reaction J (−0.4 μhartree) at B3LYP/cc-pVTZ(df-pVTZ) level of theory arise from error cancellation.

To test for auxiliary BSSE, we corrected the interaction energies of H, I, and K at the B3LYP/cc-pVTZ(df-pVTZ) level of theory by applying the CP correction. Interaction energies are defined as the difference between a molecular energy and the sum of the fragment energies with the fragments at the same geometries as in the molecule. Interaction energies thus differ from reaction energies in that the fragment geometries are not relaxed.

For reactions H and I, the fitting errors in the overlap metric of the resulting CP-corrected interaction energies are reduced from 18 to 0.6 μhartree and from 17 to −2 μhartree, respectively. By contrast, for reaction K, the fitting error increases slightly in magnitude, from 11 to −14 μhartree, when the CP correction is included. Thus, when density fitting is performed in the overlap metric, the auxiliary BSSE clearly influences the quality of reaction energies, in agreement with the discussion of the atomization energies. We stress that specifically tuned auxiliary basis sets are expected to reduce the effect of BSSE. Even with the auxiliary basis sets used here, the absolute error in the reaction energies because of density fitting in the overlap metric does not exceed 90 μhartrees.

TABLE III. Timings for a complete HF/cc-pVTZ(df-pVTZ) calculation of the naphthalene molecule. The calculation converged in 14 SCF iterations.

Method	Initialization (s)	Coulomb (s/iter)	exchange (s/iter)
J-engine+LinK		408	1394
Coulomb and exchange fitting	269	1.2	33.1

TABLE IV. Sparsity of fitting integrals in the overlap and Coulomb metrics at different thresholds τ for the acene-5 molecule of Ref. 28 in the cc-pVTZ(df-pVTZ) basis. Also listed is the ratio between the sparsities of the overlap and Coulomb integrals. The prime on the auxiliary basis-set index denote an orthogonal basis.

Integral	$\tau=10^{-10}$	$\tau=10^{-8}$	$\tau=10^{-6}$
$(\alpha\|\beta)$	52%	52%	47%
$\langle\alpha\beta\rangle$	16%	14%	11%
Ratio $\langle\alpha\beta\rangle/(\alpha\|\beta)$	0.31	0.27	0.23
$(ab\|\alpha)$	26%	21%	15%
$\langle ab\alpha\rangle$	7.5%	5.4%	3.2%
$c_\alpha^{ab}=\langle ab\beta\rangle\langle\beta\alpha\rangle^{-1}$	25%	20%	13%
Ratio $\langle ab\alpha\rangle/(ab\|\alpha)$	0.29	0.25	0.22
Ratio $c_\alpha^{ab}/(ab\|\alpha)$	0.95	0.93	0.86
$(ab\|\alpha')$	26%	21%	15%
$c_{\alpha'}^{ab}=\langle ab\alpha'\rangle$	21%	14%	6.4%
Ratio $\langle ab\alpha'\rangle/(ab\|\alpha')$	0.80	0.64	0.42

D. Timings and sparsity

The purpose of this paper is mainly to show that it is possible to perform density fitting in local metrics rather than than in nonlocal Coulomb metric. However, to illustrate that this method is indeed practicable; we present some timings and sparsity results.

As is well known, the application of integral fitting to the calculation of Coulomb and exchange matrices provides a dramatic speed-up of the calculations. Table III contains timings for a B3LYP/cc-pVTZ(df-pVTZ) calculation on naphthalene, with and without density fitting, using a development version of DALTON.[31] The calculation was carried out on a 2200 MHz SUN X2200 AMD Opteron machine, and the code was compiled with ifort 9.0 linked with mkl-libraries (version 8.1). For both Coulomb and exchange matrices, the evaluation is accelerated by almost a factor of 30. The initialization step of 269 s consists of the following main contributions: three-center integral evaluation $(ab|\alpha)$ (89 s), calculation of the inverse square root $(\alpha|\beta)^{-0.5}$ (12 s), and transformation to the orthonormal basis (164 s). The remaining 5 s consists of calculating $g_\alpha^w=\sqrt{(\alpha|\alpha)}$, $g_{ab}^w=\sqrt{(ab|ab)}$, and, after renormalization of the auxiliary basis, the $(\alpha|\beta)$ integrals.

Table IV lists the sparsity of two- and three-center integrals for acene $(n=5)$ of Ref. 28, in the Coulomb and the overlap metrics. Sparsity is listed at different screening thresholds (τ). Also listed are the ratios between the number of integrals in the overlap and Coulomb metrics. The numbers of significant two- and three-center integrals are reduced by a factor of 3–4 in the overlap metric compared to the Coulomb metric. The fitting coefficients c_α^{ab} as obtained in the overlap metric show only a slow onset of sparsity in the nonorthogonal auxiliary basis, reducing the number of significant fitting coefficients in the overlap metric by 5%–14%, for thresholds in range of 10^{-10}–10^{-6} hartree. In the orthogonal basis, the sparsity in the fitting coefficients $c_{\alpha'}^{ab}$ is maintained, reducing the number of significant fitting coefficients by 20%–58%.

VI. CONCLUSIONS AND OUTLOOK

In this paper, we have studied the variational density-fitting technique for the calculation of Coulomb and exchange matrices, with emphasis on the locality of the fitting metric. Such local metrics yield a sparse linear set of equations for the fitting coefficients, allowing for their determination in time proportional to the system size. We have shown that local metrics can be chosen such that the accuracy of the calculation does not suffer as demonstrated by our test implementation. In the derivation of the formulas, we have paid special attention to aspects of density fitting relevant for property calculations (variation principle, etc.).

ACKNOWLEDGMENTS

This work was supported by the Norwegian Research Council through the CeO Centre for Theoretical and Computational Chemistry (Grant No. 179568/V30) and through a Strategic University Program in Quantum Chemistry (Grant No. 154011/420).

[1] A. Sodt, J. E. Subotnik, and M. Head-Gordon, J. Chem. Phys. **125**, 194109 (2006).
[2] F. Weigend, Phys. Chem. Chem. Phys. **4**, 4285 (2002).
[3] F. Weigend, J. Comput. Chem. **29**, 167 (2008).
[4] J. L. Whitten, J. Chem. Phys. **58**, 4496 (1973).
[5] E. J. Baerends, D. E. Ellis, and P. Ros, Chem. Phys. **2**, 41 (1973).
[6] J. A. Jafri and J. L. Whitten, J. Chem. Phys. **61**, 2116 (1974).
[7] B. I. Dunlap, J. W. D. Connolly, and J. R. Sabin, J. Chem. Phys. **71**, 3396 (1979).
[8] B. I. Dunlap, J. W. D. Connolly, and J. R. Sabin, J. Chem. Phys. **71**, 4993 (1979).
[9] R. T. Gallant and A. St-Amant, Chem. Phys. Lett. **256**, 569 (1996).
[10] P. Sałek, S. Høst, L. Thøgersen, P. Jørgensen, P. Manninen, J. Olsen, B. Jansik, S. Reine, F. Powlowski, E. Tellgren, T. Helgaker, and S. Coriani, J. Chem. Phys. **126**, 114110 (2007).
[11] C. Fonseca Guerra, J. G. Snijders, G. te Velde, and E. J. Baerends, Theor. Chem. Acc. **99**, 391 (1998).
[12] W. T. Yang and T.-S. Lee, J. Chem. Phys. **103**, 5674 (1995).
[13] B. I. Dunlap, J. Mol. Struct.: THEOCHEM **501**, 221 (2000).
[14] O. Vahtras, J. Almlöf, and M. W. Feyereisen, Chem. Phys. Lett. **213**, 514 (1993).
[15] Y. Jung, A. Sodt, P. M. W. Gill, and M. Head-Gordon, Proc. Natl. Acad. Sci. U.S.A. **102**, 6692 (2005).
[16] R. Polly, H.-J. Werner, F. R. Manby, and P. J. Knowles, Mol. Phys. **102**, 2311 (2004).
[17] J. Pipek and P. G. Mezey, J. Chem. Phys. **90**, 4916 (1989).
[18] A. Sodt and M. Head-Gordon, J. Chem. Phys. **128**, 104106 (2008).
[19] M. A. Watson, P. Sałek, P. Macak, and T. Helgaker, J. Chem. Phys. **121**, 2915 (2004).
[20] E. Schwegler and M. Challacombe, J. Chem. Phys. **105**, 2726 (1996).
[21] C. Ochsenfeld, C. A. White, and M. Head-Gordon, J. Chem. Phys. **109**, 1663 (1998).
[22] F. Aquilante, T. B. Pedersen, and R. Lindh, J. Chem. Phys. **126**, 194106 (2007).
[23] B. Jansík, S. Høst, P. Jørgensen, J. Olsen, and T. Helgaker, J. Chem. Phys. **126**, 124104 (2007).
[24] T. Helgaker, P. Jørgensen, and J. Olsen, *Molecular Electronic-Structure Theory* (Wiley, Chichester, 2000).
[25] L. E. McMurchie and E. R. Davidson, J. Comput. Phys. **26**, 218 (1976).
[26] C. C. M. Samson, W. Klopper, and T. Helgaker, Comput. Phys. Commun. **149**, 1 (2002).
[27] S. Reine, E. Tellgren, and T. Helgaker, Phys. Chem. Chem. Phys. **9**, 4771 (2007).
[28] M. J. G. Peach, P. Benfield, T. Helgaker, and D. J. Tozer, J. Chem. Phys. **128**, 044118 (2008).
[29] S. F. Boys and F. Bernardi, Mol. Phys. **19**, 553 (1970).
[30] Y. Zhao and D. G. Truhlar, Theor. Chem. Acc. **120**, 215 (2008).
[31] DALTON, an ab initio electronic structure program, Release 2.0, 2005 (see http://www.kjemi.uio.no/software/dalton/dalton.html).